Materials for Renewable and Sustainable Energy (2018) 7:15
https://doi.org/10.1007/s40243-018-0122-z

ORIGINAL PAPER

Properties of activated MgH_2 + mischmetal nanostructured composite produced by ball-milling

Mohammad Amin Rahmaninasab[1] · Shahram Raygan[1] · Hossein Abdizadeh[1] · Mahdi Pourabdoli[2] · Seyyed Hamed Mirghaderi[1]

Received: 25 February 2018 / Accepted: 23 May 2018 / Published online: 29 May 2018

Abstract
MgH_2 + mischmetal nanostructured composite was synthesized from MgH_2 plus 6 and 10 wt% of mischmetal by ball-milling at various times. XRD studies revealed that cerium hydride was produced during the milling in all samples. Sievert test results indicated that the samples containing 6 wt% of mischmetal showed a higher desorption compared with the ones containing 10 wt% of mischmetal. The high amount of cerium hydride in the samples may be the reason, while hydrogen desorption properties decreased by adding more catalyst. Furthermore, BET results showed that the addition of the catalyst to the samples resulted in agglomerate formation in shorter milling times. The agglomerate formation increased with adding more amounts of mischmetal, thus decreasing the hydrogen desorption properties of the composite. The best results were obtained from the 30 h-milled sample containing 6 wt% of catalyst. The on-set desorption temperature of this sample was 100 °C lower than that of as-received MgH_2.

Keywords Magnesium hydride · Milling · Catalyst · Mischmetal · Hydrogen storage

Introduction

Supplying energy through fossil fuels creates challenges such as global warming and climate change due to the emission of greenhouse gases, pollution of urban areas, and reduction of oil resources [1]. Because of its abundance and lack of contamination, hydrogen is among the best options for replacing fossil fuels. Finding a safe method for hydrogen storage is one of the challenges of using hydrogen as a new fuel. Hydrogen can be stored as a pressurized gas, liquid gas, and as solid-state hydrogen in materials such as magnesium hydride (MgH_2) [2]. The storage of hydrogen in the form of reversible metal hydrides is the main alternative for low-capacity methods such as storage under pressure or in liquid form at low temperatures. Hydrides have the potential to store hydrogen in low-volume reservoirs without disadvantages such as the need for low temperature in liquid storages or hazards and inefficiencies in the pressurized gas method.

Extensive research on magnesium and its alloys for use as hydrogen storage has been carried out due to its high storage capacity and low price [3]. Magnesium-based hydrides also have good application properties such as thermal resistance, reversibility, and recycling capability. Hence, in recent years, more attention has been paid to research on magnesium and its alloys. MgH_2 has a high hydrogen storage capacity of 7.7 wt% with low production costs due to its abundance and recyclability [4].

The hydrogen desorption temperature of MgH_2 is 327 °C under the hydrogen pressure of 1 bar. However, various temperatures of more than 400 °C have also been reported depending on the activation process of MgH_2. Although this temperature is lower than that of other hydrides, it is extremely high for practical applications [5]. The main disadvantages of MgH_2, as a hydrogen storage medium, are its high hydrogen desorption temperature, slow kinetics of hydrogen absorption, and high tendency to react with oxygen [6]. These problems can be solved by methods such as mechanical milling and catalyst addition.

✉ Shahram Raygan
shraygan@ut.ac.ir

[1] School of Metallurgy and Materials Engineering, College of Engineering, University of Tehran, Tehran, Iran

[2] Department of Material Engineering, Hamedan University of Technology, Hamadan, Iran

One of the most common methods for improving the sorption of hydrogen from magnesium hydrides is ball-milling. Mechanical milling increases the free surface, creates micro/nanostructures, enhances grain boundaries, decreases grain size, creates a porous surface structure with high active sites for the adsorption and desorption of hydrogen, creates micro-strains, and forms defects on the surface or inside the material. The created defects encourage the diffusion of hydrogen into the material by decreasing the diffusion activation energy. Milling also changes the microstructure and size of magnesium/magnesium hydride crystals and grains, exerting a great influence on the sorption of hydrogen. These factors improve kinetics and surface activation to absorb or desorb hydrogen, decrease the activation energy, reduce the temperature of desorption, and improve kinetics and hydrogen diffusion in the material. As already mentioned, milling reduces the size of grains and crystallites. These two factors have a great influence on the kinetics of hydrogen absorption/desorption. A smaller crystallite size is proportional to more grain boundaries. Due to the low density of atoms in grain boundaries, the diffusion of hydrogen is usually faster in grain boundaries than inside grains. In addition, grain boundaries are suitable nucleation sites for the formation or decomposition of the hydride phase. Reducing the crystallite size of the powder material increases the surface area and decreases the length of the hydrogen diffusion path. The area is proportional to the rate of surface reaction with hydrogen, while the length of the hydrogen diffusion path is proportional to the kinetics of hydride formation or decomposition [7–10]. Wagemans et al. [11] investigated the hydrogen desorption properties of MgH_2 using quantum mechanical calculations and found that MgH_2 clusters with nanoscale dimensions had a significantly lower (63 kJ/mol) desorption enthalpy than MgH_2. Thus, hydrogen desorption occurs at lower temperatures for nano-sized magnesium clusters. The desorption temperature of magnesium clusters (with the approximate size of 0.9 nm) is calculated only at 200 °C. It is reported that ball-milling also increases the rate of hydrogen absorption and desorption from MgH_2 by removing the oxide layers on the surface [12].

The use of catalysts is one way to improve surface kinetics. Therefore, different catalysts such as metal oxides, intermetallic compounds, and carbon materials have been used to improve the properties of hydrides [3–7]. The desirable catalytic effect of metals and their oxides has also been demonstrated on hydrogen desorption/absorption in magnesium-based hydrides. Liang et al. [13] mixed MgH_2 with titanium, vanadium, manganese, iron, and nickel through mechanical milling. All the added elements reduced the activation energy of hydrogen desorption from MgH_2. The MgH_2–vanadium composite showed the fastest kinetics of desorption and its activation energy (62.3 kJ/mol) was much less than that of MgH_2 (120 kJ/mol). Meanwhile, the composite containing titanium demonstrated the fastest absorption kinetics. The added elements helped combine hydrogen atoms in a catalytic reaction. The catalytic activity of the added elements was influenced by the high number of structural defects, low compound stability, chemical composition of the intermediate metal ions in the composition, and high prevalence of hydrogen ion–metal ions [14]. High-energy ball-milling also plays a role in the synthesis of hydrides and catalysts composites, creating a good interface between hydride and catalyst and promoting the proper distribution of the catalyst [15].

The enthalpy of hydrogenation reaction can be reduced by alloying magnesium with some elements. Thus, alloying is a traditional and efficient solution for improving the thermodynamics of hydrogen absorption and desorption from magnesium. As an example, Ni_2Mg can react with hydrogen and form Mg_2NiH_4. The hydrogenation enthalpy of Mg_2NiH_4 (− 64.5 kJ/mol) is less than the enthalpy of MgH_2 formation (− 75 kJ/mol) [10]. Morinaga et al. [16] found that the binding energy between hydrogen and nickel is stronger than that of magnesium in Mg_2NiH_4. This nickel–hydrogen bond in Mg_2NiH_4 is weaker than that of magnesium and hydrogen in pure MgH_2, resulting in the low formation enthalpy of Mg_2NiH_4. Magnesium and copper can create a Cu_2Mg alloy. During the absorption of hydrogen, Cu_2Mg is decomposed into MgH_2 and $MgCu_2$ and the equilibrium temperature of hydrogen desorption under 1 bar H_2 pressure decreases to 240 °C. However, this reaction is not reversible [12].

In this research, the nanostructured composite of MgH_2–mischmetal was prepared by ball-milling to investigate the simultaneous effect of milling and addition of mischmetal as a catalyst. Findings of various studies have revealed that some elements have a good catalytic effect on the process of hydrogen absorption and desorption from MgH_2. Nevertheless, few studies have been conducted on the effect of rare earth elements on the hydrogen desorption properties of MgH_2. Therefore, a combination of cerium and lanthanum transition metals (mischmetal) as the catalyst was employed in this study.

Materials and research process

In this study, MgH_2 (Alfa Aesar < 140 μm, purity > 95%) and small slices cut from a bulk of mischmetal containing 65.37 wt% of cerium, 34.37 wt% of lanthanum, 0.1 wt% of neodymium, and 0.1 wt% of praseodymium were utilized as raw materials. MgH_2 was ball-milled for 10, 30, and 40 h to examine the effect of ball-milling on the properties of the used powder. To prepare the nanostructured composite, 3 g of MgH_2 powder with the addition of 6 wt% of mischmetal was ball-milled for 10, 20, 30, and 40 h. Moreover, to study the effect of the amount of catalyst on the hydride properties of the nanostructured composites, 10 wt% of mischmetal

was added to 3 g of MgH_2 powder and then ball-milled for 20 and 30 h.

Ball-milling was performed in a high-energy planetary ball mill (PM2400 Asia Rakhsh Co.) using a hardened chromium-nickel steel (150 mL) vial and hardened steel balls (5, 10, and 20 mm in diameter) with ball to powder weight ratio of 20 and rotation speed of 250 rpm under argon atmosphere. It is reported that, in ball-milling, different ball sizes are sometimes mixed to randomize the motion of balls and increase the efficiency of milling [17]. After the completion of the ball-milling process, the vial was opened in a glove box under high-purity argon gas to prevent the oxidation of samples.

To recognize and analyze the phases, X-ray diffraction (XRD) (Philips X'Pert Pro diffractometer) with CuK_α radiation, at the wavelength of $\lambda = 0.1541874$ nm, in the range of $2\theta = 20$–$100°$, and step size of 0.02° was used. The X'Pert HighScore Plus v2.2b software of PANalytical Company was employed to identify the phases. Mean crystallite size and the lattice micro-strain of the particles were measured using the Williamson–Hall method [18]:

$$\beta_{\text{sample}} \cos\theta = K\lambda/\delta + 2\varepsilon \sin\theta, \quad (1)$$

where β_{sample} is the full width at half maximum (FWHM) of the milled powder, θ is the position of peak maximum, K is the Scherrer constant (about 0.9), λ is the beam wavelength, δ is the crystallite size, and ε is the lattice micro-strain introduced by ball-milling. For instrumental correction, a Gaussian relationship was used [19]:

$$\beta_{\text{sample}} = \sqrt{\beta^2_{\text{experimental}} - \beta^2_{\text{instrumental}}}, \quad (2)$$

where $\beta_{\text{experimental}}$ is the measured FWHM of the annealed nickel powders.

To explore the morphology of the samples, a Tescan-MV 2300 scanning electron microscope and Zeiss-Sigma field-emission scanning electron microscope were utilized. Particle size was calculated using the MIP image analysis software in the form of a circle diameter equal to the particle size $ECD = (4A/\pi)^{1/2}$. In this formula, A represents the magnitude of the surface of the particle. Particle size was determined by several images and by specifying 300–700 particles in each measurement. To measure the free surface of the samples (BET test), the BELSORP-mini II device with liquid nitrogen was used. Before BET experiments, the samples were heated up to 180 °C and maintained for 4 h to remove all possible moisture. The main parameters were 195.65 °C for 55 min and 10 points BET measurement. To measure the properties of hydrogen desorption, a homemade Sievert apparatus was employed. Before the experiments, all the samples were subjected to activation using a Sievert machine under the hydrogen pressure of 4 Mpa at 180° C for 4 h. A sample of 300 mg was placed in the Sievert apparatus and washed with argon gas. The samples were then heated up to 500 °C with the rate of 10 °C/min. Finally, the results were reported as the curve of the amount of hydrogen desorbed versus temperature. All Sievert tests were performed at least twice to ensure reproducibility.

Results and discussion

Phase identifying

Figures 1 and 2 depict the XRD patterns of mischmetal and MgH_2, respectively. In Fig. 2, low-intensity magnesium peaks are observed, which were predictable according to the > 95 wt% purity of primary MgH_2.

Figure 3 illustrates the XRD patterns of as-received MgH_2 and ball-milled MgH_2. According to these patterns, increasing the milling time increased the width and reduced the intensity of the peaks. Moreover, some of the

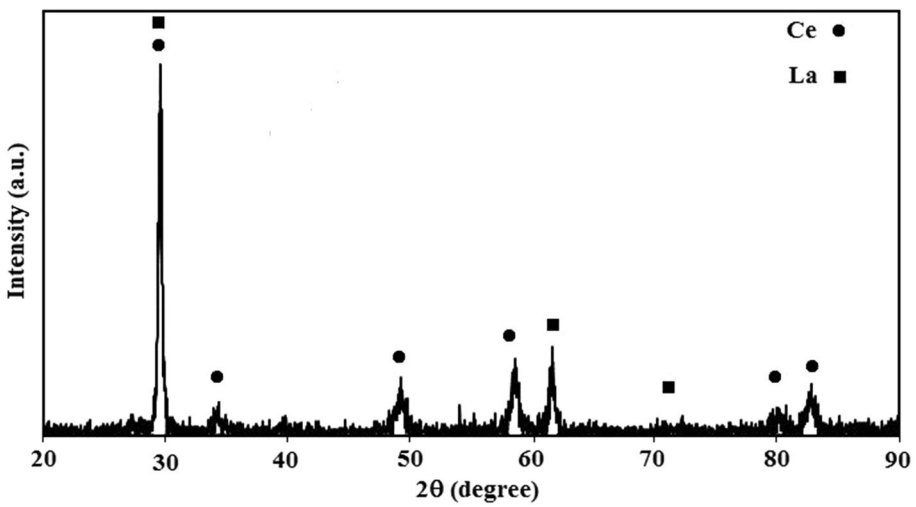

Fig. 1 XRD pattern of the mischmetal used in this study

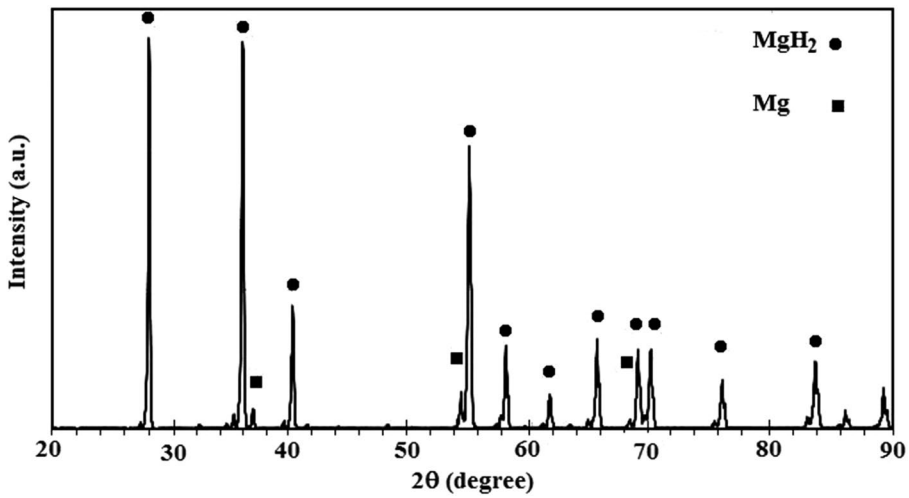

Fig. 2 XRD pattern of the magnesium hydride used in this study

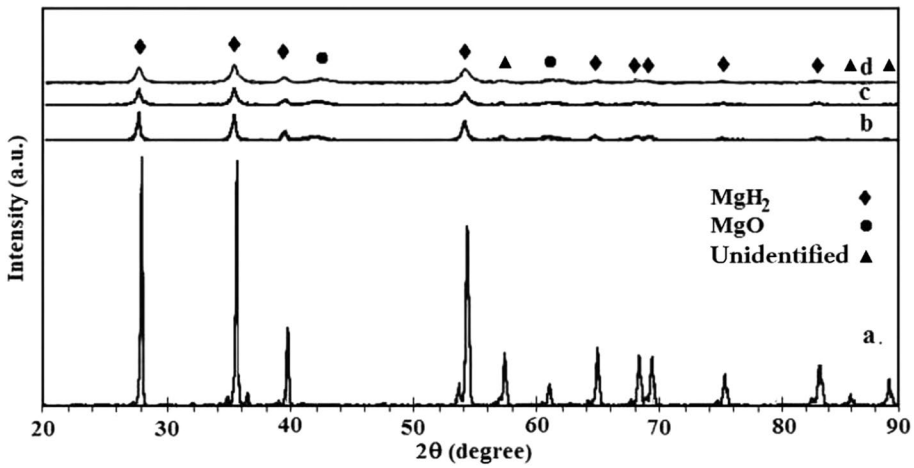

Fig. 3 XRD patterns of **a** as-received MgH_2 and MgH_2 milled for **b** 10, **c** 30, and **d** 40 h

weak peaks disappeared by increasing the milling time due to the reduction of crystallite size as well as the increase in lattice strain and internal energy during milling [20]. In the ball-milled samples, a weak peak was observed from magnesium oxide. The formation of this compound may be due to the presence of Mg in the initial MgH_2 and tendency towards oxidation during ball-milling. It is well-known that ball-milled powders are very active. One reason for the oxidation of active Mg during ball-milling may be the presence of oxygen as an impurity in the flowing argon gas especially when the majority of argon in the gas container is used and the amount of gas in the container is less than 1/4 of container volume. Another reason can be the leakage of glove box and entrance of oxygen into it. Oxidation can also be performed during the movement of samples from the laboratory towards the XRD machine.

Table 1 shows the variation of crystallite size and lattice strain of MgH_2 with ball-milling. It can be observed that crystallite size was reduced from 87 nm for the unmilled powder to 32 nm for the 40 h-milled MgH_2, and lattice strain increased to 1.07% due to the 40 h milling.

Table 1 Mean crystallite size and lattice strain of the ball-milled MgH_2

Time of ball-milling (h)	Mean crystallite size (nm)	Lattice strain (%)
0	87	–
10	58	0.72
30	35	0.95
40	32	1.07

Morphology of ball-milled MgH_2

The SEM images of as-received MgH_2 and ball-milled MgH_2 (10, 30, and 40 h) are depicted in Fig. 4. Based on Fig. 4b, after 10 h of milling, MgH_2 particles became spherical and their mean size reached 338 nm. The presence of

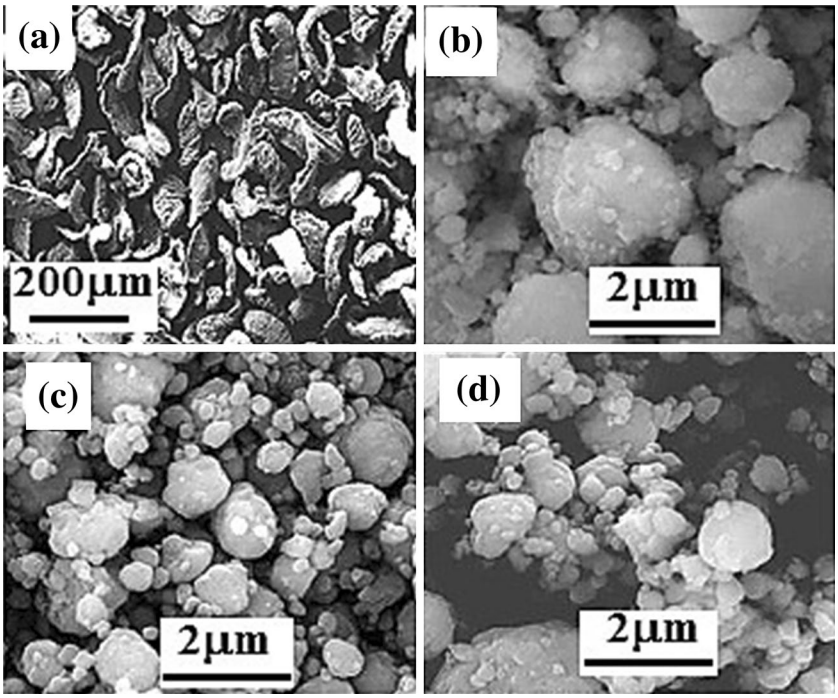

Fig. 4 Scanning electron microscopy (SEM) images of **a** as-received MgH_2 and MgH_2 ball-milled for **b** 10, **c** 30, and **d** 40 h

small particles along with the coarse particles or agglomerate of particles in the sample milled for 10 h shows the non-uniform distribution of particle size in this sample. With an increase in ball-milling time from 10 to 30 h, the particles were slightly smaller and the mean size of the particles reached 306 nm. An increase in the ball-milling time up to 30 h also led to a more uniform distribution of the particle size. The particles were agglomerated in the sample milled for 40 h and the mean size of the particles increased to 372 nm. After milling for a certain period, a state of equilibrium was created and fine particles became larger, while coarse particles became smaller due to the balance between the cold-welding rate (which tended to increase the mean particle size) and the rate of fracture (that led to reduce the mean particle size). The mean particle size eventually reached to the equilibrium size [21]. It can be assumed that no reduction in the mean particle size would be observed at longer milling times.

Effect of ball-milling on the hydrogen desorption properties of MgH_2

The results of hydrogen desorption studies on as-received and ball-milled MgH_2 (10, 30, 40 h) are illustrated in Fig. 5. The on-set desorption temperature of MgH_2 decreased from 480 °C for as-received MgH_2 to 400 °C for 40 h-milled MgH_2 in the condition of these experiments. The on-set desorption temperature of as-received MgH_2 has been reported to be above 300 °C [1, 5]. The reason for the difference in temperature measured in this study with the reported

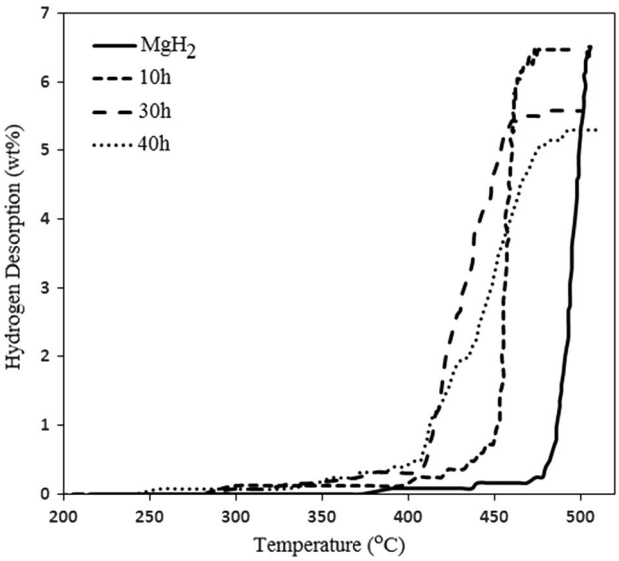

Fig. 5 Hydrogen desorption behavior of as-received MgH_2 and ball-milled MgH_2 for 10, 30, and 40 h

temperature can be the surface oxidation and the need for more activation. However, due to the uniformity of activation conditions for all samples, the results are comparable with each other. The difference between the on-set desorption temperature of as-received MgH_2 and 40 h ball-milled MgH_2 (400 and 480 °C) is the increased specific surface area and lattice strain, reduced size of crystallites, and formation of structural defects in the material, which facilitate hydrogen desorption. The positive role of milling in reducing

the hydrogen desorption temperature has been confirmed. Nevertheless, with increasing the milling time from 30 to 40 h, the desorption curve slightly shifted to the right (higher temperature), perhaps due to the agglomeration of particles and reduction of their free surface area. Therefore, to further decrease the temperature of hydrogen desorption, the catalyst was added to MgH_2 prior to the milling process.

Effect of catalyst addition on MgH_2

Phase identifying of MgH_2: 6 wt% of mischmetal

The XRD patterns of MgH_2 ball-milled for 10 h as well as the MgH_2 containing 6 wt% of mischmetal milled for 10, 20, 30, and 40 h are shown in Fig. 6. By comparing the XRD patterns of MgH_2 milled for 10 h and MgH_2 containing 6 wt% of mischmetal milled for 10 h, a broadening and decrease in the peak intensities of the catalyst-containing sample can be observed. This is due to the decrease in crystallite size and increase in lattice strain through the addition of catalyst (mischmetal). Catalyst particles can act as hard balls during milling and contribute to structural defects [22].

Peaks of $CeH_{2.73}$ were observed in the catalyst-containing samples. Considering the lower Gibbs free energy of formation for cerium hydride (-204.8 kJ/mol H_2) in comparison with MgH_2 (-75 kJ/mol H_2), it seems that cerium reacted with MgH_2 during high-energy ball-milling according to Eq. 3 and formed cerium hydride [23].

$$Ce + MgH_2 \rightarrow CeH_2 + Mg \ \Delta G_f^{\circ} = -129.8 \text{ kJ/mol}. \quad (3)$$

Due to the non-equilibrium nature of the milling process, the formation of non-stoichiometric hydrides of cerium such as $CeH_{2.73}$ was also expected. Figure 7 shows the diffraction pattern of a sample containing 6 wt% of mischmetal which was ball-milled for 30 min. It was observed that the intensity of the cerium hydride peak was low, indicating the formation of a low amount of this compound at short milling times. However, as the milling time increased, the intensity of the cerium hydride peak increased in the samples. It can be concluded that an increment in the milling time led to a higher amount of hydride in the samples. Cerium hydride may be formed on the surface of cerium. It has been reported that this surface layer controls the reaction rate of the formation of cerium hydride [24]. Creating new surfaces and fracture of cerium hydride layers on the surface of cerium due to mechanical milling facilitates the formation of cerium hydrides. The formation of hydrides during the milling process has also been reported by Shang et al. [23]. This layer also affects the amount of hydrogen desorption from the powder mixture.

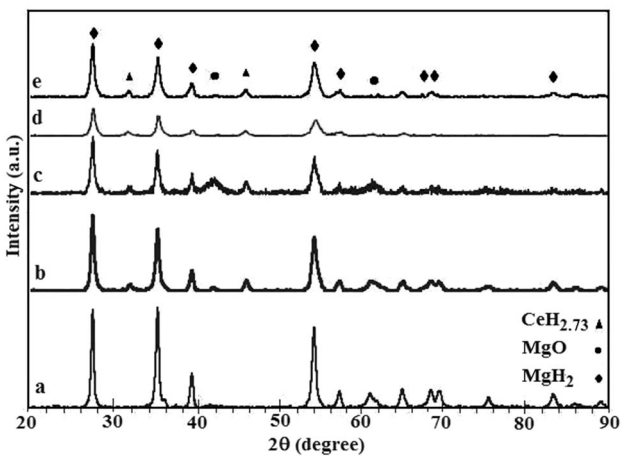

Fig. 6 The XRD pattern of **a** 10 h ball-milled MgH_2 and MgH_2-6wt % of mischmetal ball-milled for **b** 10 h, **c** 20 h, **d** 30 h, and **e** 40 h

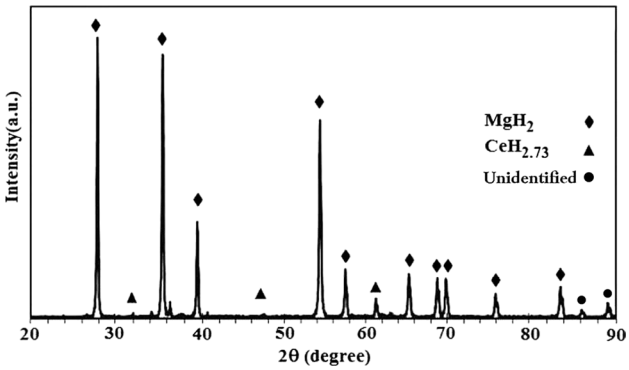

Fig. 7 The XRD pattern of 30 min ball-milled MgH_2-6 wt% of mischmetal

Particle morphologies

Figure 8 shows the SEM images of MgH_2-6 wt% of mischmetal ball-milled for 10, 20, 30, and 40 h. It has been reported in Sect. 2.2 that the mean particle size of the 10 h ball-milled MgH_2 is 338 nm, while the particle size of the 10 h ball-milled MgH_2-6 wt% of mischmetal is 287 nm. By increasing the milling time of MgH_2-6 wt% of mischmetal from 10 to 20 h, the particle size increased and the mean particle size reached 381 nm. In the 30 h-milled sample, the mean particle size was 360 nm. At shorter milling times, large and small particles were created together. However, with increasing the milling time and approaching the equilibrium level, small particles stuck together and large particles broke into small ones [21]. The increased particle size in the 20 h-milled sample can be attributed to the agglomeration of fine particles and reduction of particle size in the 30 h-milled sample can be due to the fracture of large particles. By increasing this time to 40 h, the particles stuck together and agglomerated with the mean size of 417 nm. By

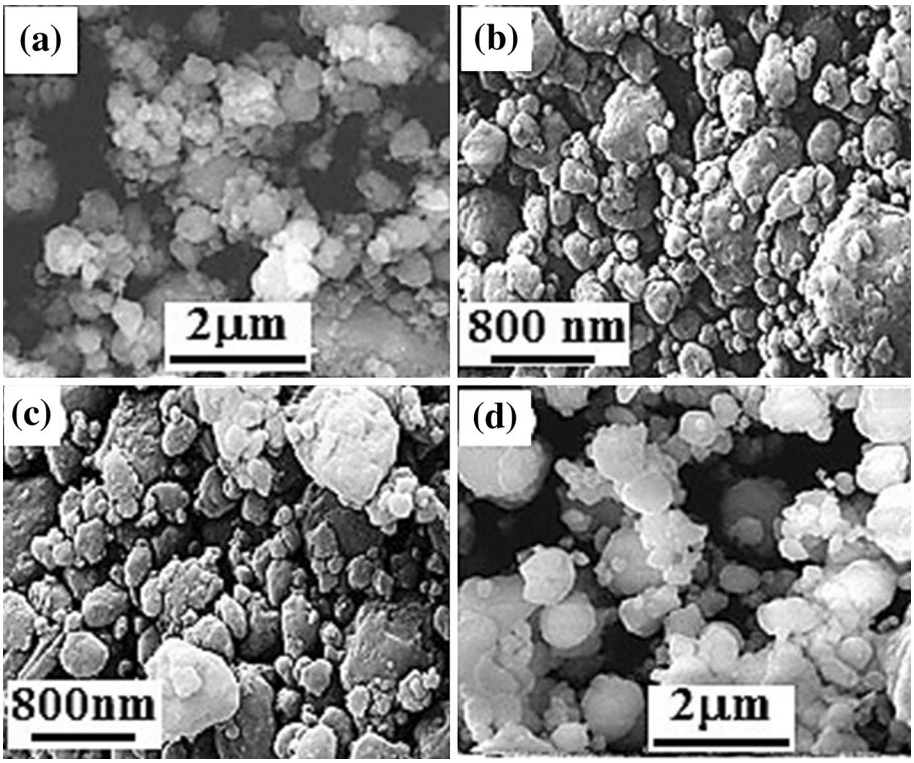

Fig. 8 The SEM images of MgH_2-6 wt% of mischmetal ball-milled for **a** 10, **b** 20, **c** 30, and **d** 40 h

comparing these results with those of the samples without a catalyst, it can be seen that smaller particles were achieved in short ball-milling times by adding the catalyst. This can be attributed to the role of the catalyst in the application of more work on particles, resulting in cold-welding and particle-bonding [21].

Determination of specific surface area (BET)

Free surface changes, mean porosity diameter, and mean pore volume for the MgH_2 samples milled for 10 h and the MgH_2 samples with 6 wt% of catalyst milled for 10, 20, 30, and 40 h are shown in Fig. 9. According to these diagrams, the sample with the catalyst that is milled for 10 h has the highest free surface with the smallest mean diameter of porosity and the highest pore volume. By comparing the MgH_2 sample milled for 10 h with the MgH_2 sample with the catalyst milled for 10 h, it can be observed that the addition of the catalyst increased the free surface and mean pore volume, but decreased the pore size. It can be concluded that the addition of the catalyst led to a smaller particle size, which is also confirmed by SEM images. By increasing the milling time to 20 h for the catalyst containing MgH_2, the free surface area and mean pore volume decreased and the mean diameter of the pores increased. According to the results of SEM images, it can be concluded that the closing and mixing of the porosities occurred simultaneously with the particle size increase, and hence the free surface loss was observed. The increase in the milling time up to 30 h led to the fracture of large particles, resulting in an increase in free surface relative to the 20 h-milled sample. During the ball-milling process, the removing, mixing and shrinkage of pores and forming new porosities occurred simultaneously by agglomeration of new particles [21]. According to the results of the BET test, it seems that the agglomeration and removal of porosities resulted in a reduced free surface and mean pore volume in the 40 h ball-milled MgH_2-6 wt% of mischmetal sample.

Hydrogen desorption properties

Figure 10 illustrates the results of the hydrogen desorption of MgH_2, MgH_2 milled for 10 h, and MgH_2 with 6 wt% of catalyst milled for 10, 20, 30, and 40 h. By comparing the MgH_2 samples milled for 10 h with MgH_2 with the catalyst milled for 10 h, it was observed that the addition of catalyst reduced the temperature of hydrogen desorption and decreased the amount of desorbed hydrogen. The decrease in the on-set desorption temperature of hydrogen can be due to the positive effect of the catalyst on the hydrogen desorption process by increasing the free surface and accumulated energy in the milled powder and reducing the activation energy. The reduction in the amount of desorbed hydrogen can be due to the formation of the cerium hydride phase during the milling process. The cerium hydride phase formed during ball-milling was stable at high temperatures [23] and, thus,

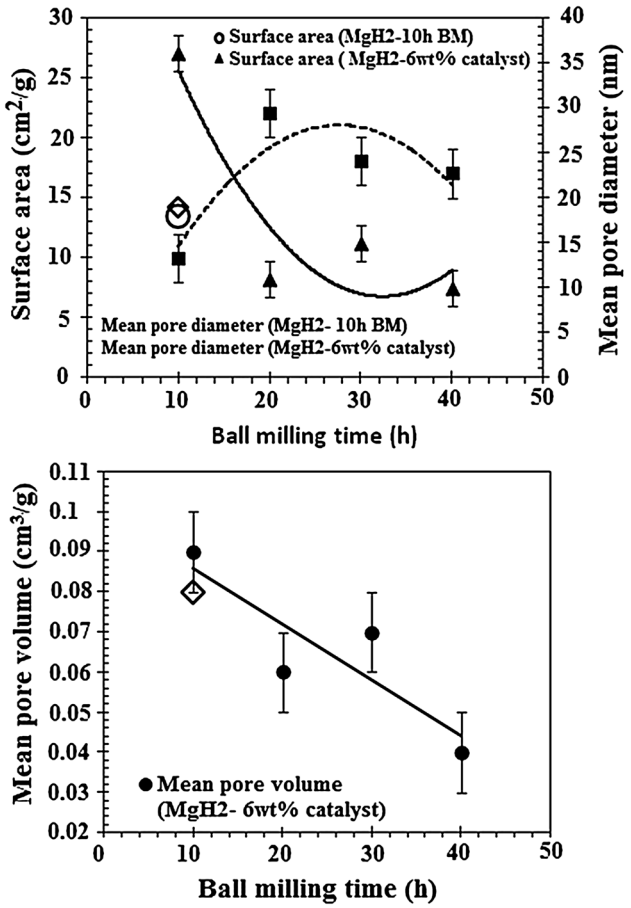

Fig. 9 Free surface, mean porosity diameter, and mean pore volume for the 10 h ball-milled MgH_2 and MgH_2-6 wt% of mischmetal ball-milled for 10, 20, 30, and 40 h

the formation of this phase reduced the amount of desorbed hydrogen from the milled MgH_2-catalyst mixture. Increasing the milling time to 20 and 30 h also reduced the temperature of hydrogen desorption. By comparing the results of MgH_2-6 wt% of mischmetal milled for 10, 20, and 30 h and considering the results of the BET test, it can be observed that the on-set desorption temperature of the sample milled for 10 h is more than that of the samples ball-milled for 20 and 30 h despite the lower free surface in the 20 and 30 h-milled mixtures. This can be attributed to the increase in the internal energy, formation of defects in the structure, and reduction in the diffusion path of hydrogen atoms. The on-set desorption temperature of hydrogen in the 40 h ball-milled sample increased compared to the 30 h ball-milled sample. This is because of the increase in particle size and free surface loss in the 40 h ball-milled sample due to the cold-welding phenomenon.

Effect of increasing the amount of the catalyst

To examine the effect of the amount of catalyst on the hydrogen desorption properties of MgH_2, the $MgH_2 + 10$ wt% of mischmetal powder mixture was prepared by ball-milling for 20 and 30 h. Figure 11 shows the X-ray diffraction patterns of the samples containing 6 and 10 wt% of catalyst which were milled for 20 and 30 h.

Table 1 also shows the crystallite size and lattice strain of MgH_2-10 wt% of mischmetal ball-milled for 20 and 30 h and MgH_2-6wt % of mischmetal ball-milled for 20 and 30 h. Similar to the samples containing 6 wt% of catalyst, cerium hydride peaks were observed in the samples containing 10 wt% of catalyst. By adding more catalyst in the same milling time, the peaks of the XRD pattern became wider.

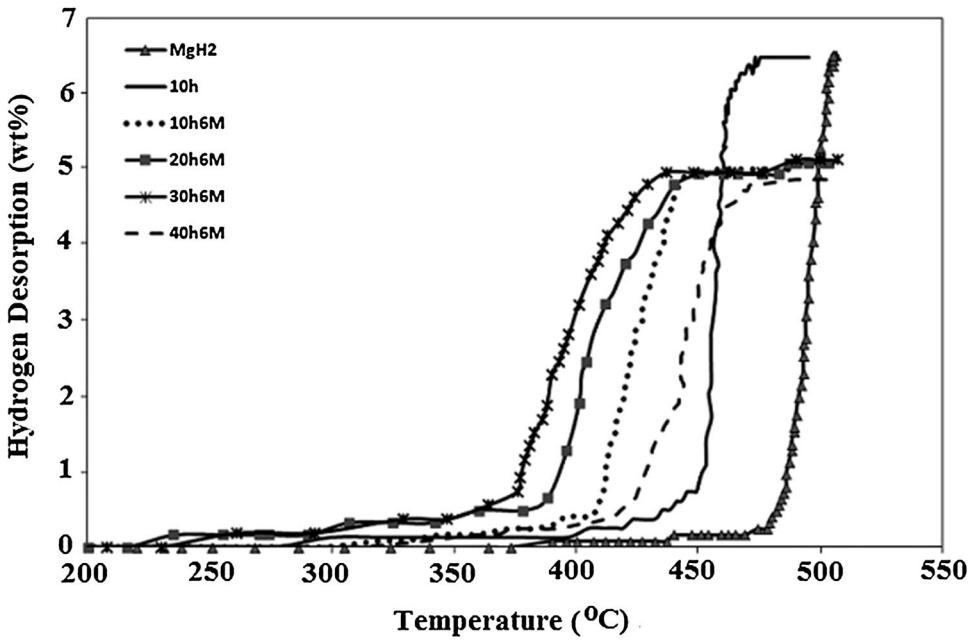

Fig. 10 Hydrogen desorption behavior of as-received MgH_2, 10 h ball-milled MgH_2, and MgH_2-6 wt% of mischmetal ball-milled for 10, 20, 30, and 40 h

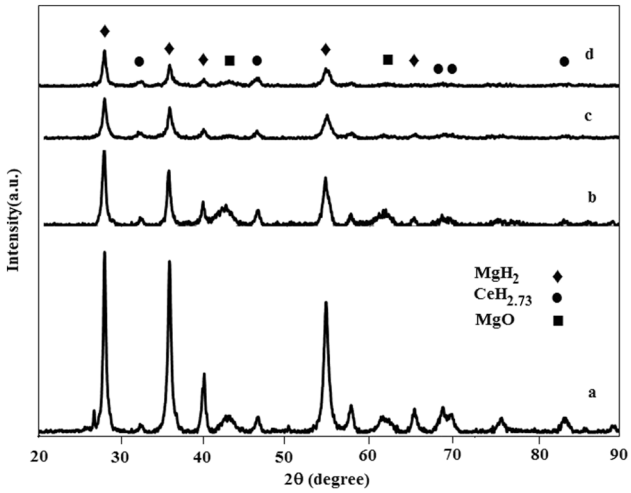

Fig. 11 XRD patterns of MgH_2-6 wt % of mischmetal ball-milled for **a** 20, **c** 30, and MgH_2-10 wt% of mischmetal ball-milled for **b** 20 and **c** 30 h

Table 2 Mean crystallite size and lattice strain of the ball-milled MgH_2-10 wt% and MgH_2-6 wt% of mischmetal after 20 and 30 h of ball-milling

Sample	Time of ball milling (h)	Mean crystallite size (nm)	Lattice strain (%)
MgH_2-6 wt% of mischmetal	20	33	1.02
MgH_2-10 wt% of mischmetal	20	33	1.08
MgH_2-6 wt% of mischmetal	30	33	1.19
MgH_2-10 wt% of mischmetal	30	30	1.65

Table 2 confirms the role of adding catalyst in creating lattice strain in crystallites in comparison with MgH_2 (Fig. 3). It is clear from Fig. 10 that adding to the amount of catalyst at a constant milling time led to more lattice strain in the samples.

According to the SEM images of MgH_2-10 wt% of mischmetal milled for 20 and 30 h in Fig. 12, the mean particle size of the 20 h-milled sample increased in comparison with the MgH_2-6 wt% of mischmetal milled for the same time. This increase in the mean particle size also showed the effect of catalyst addition on the achievement of equilibrium between cold-welding and fracture at lower times of ball-milling. Subsequently, cold-welding became the predominant process and agglomeration occurred. Thus, particle size was higher in MgH_2-10 wt% of mischmetal due to the further agglomeration. Agglomeration can also be seen in Fig. 12b for the 30 h-milled powder.

The hydrogen desorption behavior of MgH_2-6 wt% of mischmetal and MgH_2-10 wt% of mischmetal ball-milled for 20 and 30 h, and also of the 30 h-milled MgH_2 can be observed in Fig. 13. The latter sample helped understand the effect of catalyst addition. It was observed that an increase in the amount of catalyst led to a reduction in the amount of hydrogen desorption because of the further formation of cerium hydride with increase in the catalyst. Increasing the amount of catalyst from 6 to 10 wt% also resulted in a 15 °C increment in the on-set hydrogen desorption temperature of the sample milled for 20 h and a 20 °C increase in the on-set hydrogen desorption temperature of the sample milled for 30 h. Shang et al. [23] explained the rise in hydrogen desorption temperature as a result of the formation of a stable layer of cerium hydride on particle surfaces, stating that the creation of this surface layer would be problematic for the diffusion of hydrogen from inside the particles outward. This seems to be true for high amounts of cerium hydride. In addition, it is possible to consider the increase of particle size and reduction of free surface as a reason for increasing the temperature of hydrogen desorption.

Conclusion

The results of this research can be summarized as follows:

1. The XRD patterns of as-received MgH_2 and ball-milled MgH_2 show that increasing the milling time led to an increase in the width and reduction in the intensity of peaks. It is shown that crystallite size reduced from 87 nm for the unmilled powder to 32 nm for the

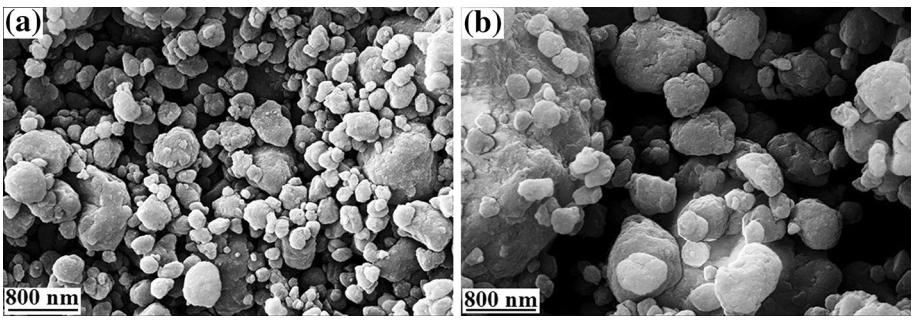

Fig. 12 SEM images of MgH_2-10 wt% of mischmetal ball-milled for **a** 20 and **b** 30 h

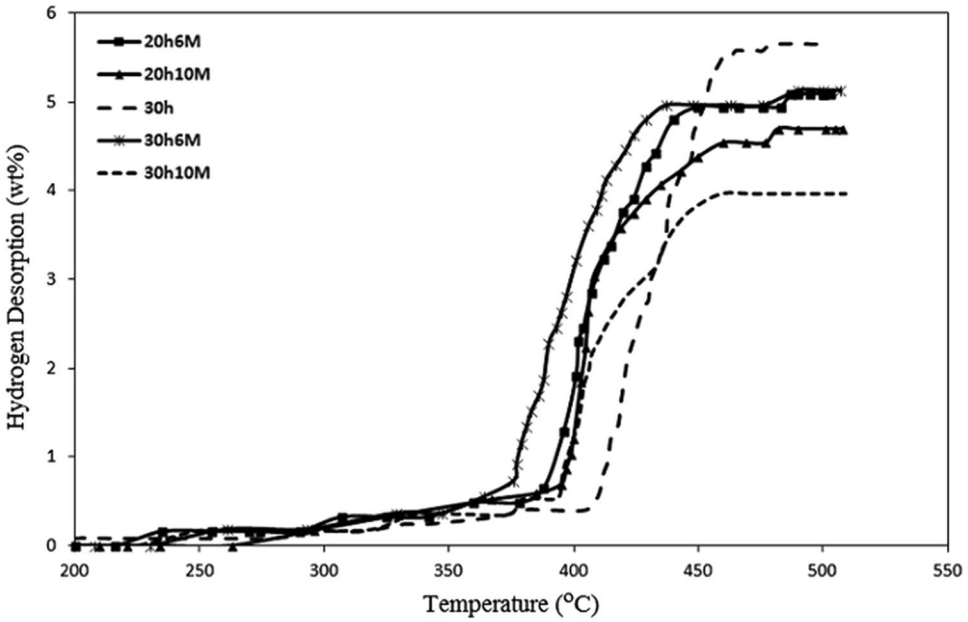

Fig. 13 Hydrogen desorption behavior of MgH_2-6 wt% of mischmetal and MgH_2-10 wt% of mischmetal milled for 20 and 30 h and also of the 30 h-milled MgH_2

40 h-milled MgH_2 and the lattice strain increased to 1.07% due to 40 h of milling.

2. Increasing the milling time up to 40 h resulted in an improvement in the hydrogen desorption properties of MgH_2 and 80 °C reduction in hydrogen desorption temperature
3. By adding the mischmetal, cerium reacted with MgH_2 during ball-milling and formed cerium hydride. It seems that the amount of this hydride increased with an increment of mischmetal from 6 to 10 wt%. This hydride was also stable at high temperatures, resulting in the harder desorption of hydrogen in large quantities.
4. Comparing the XRD results of 10 h-milled MgH_2-6 wt% of mischmetal to 10 h-milled MgH_2 revealed that crystallite size decreased and the lattice strain increased by the addition of the catalyst (mischmetal).
5. Mischmetal exhibited a suitable catalytic effect on the hydrogen desorption properties of MgH_2 and, in the best case, the reduction in hydrogen desorption temperature of the sample containing 6 wt% of mischmetal milled for 30 h was 100 °C.Therefore, the powder containing 6 wt% of mischmetal milled for 30 h is the most suitable sample from the desorption point of view.
6. Increasing the amount of mischmetal from 6 to 10 wt% led to an increment in the hydrogen desorption temperature of the milled MgH_2–mischmetal mixture.

References

1. Varin, R.A., Czujko, T., Wronski, Z.S.: Nanomaterials for solid state hydrogen storage. Springer Science & Business Media, New York (2009)
2. Ogden, J.M.: Developing an infrastructure for hydrogen vehicles: a Southern California case study. Int. J. Hydrogen Energy **24**, 709–730 (1999)
3. Grochala, W., Edwards, P.P.: Thermal decomposition of the non-interstitial hydrides for the storage and production of hydrogen. Chem. Rev. **104**, 1283–1316 (2004)
4. Alefeld, G., Volkl, J.: Topics in Applied Physics. Hydrogen In Metals. I.-Basic Properties, vol. 28. Springer, New York (1978)
5. Walker, G.: Solid-State Hydrogen Storage: Materials and Chemistry. Elsevier, Amsterdam (2008)
6. Zaluska, A., Zaluski, L., Ström-Olsen, J.: Nanocrystalline magnesium for hydrogen storage. J. Alloy Comd. **288**, 217–225 (1999)
7. Guoxian, L., Erde, W., Shoushi, F.: Hydrogen absorption and desorption characteristics of mechanically milled Mg 35 wt% FeTi1. 2 powders. J. alloy compd. **223**, 111–114 (1995)

8. Wang, P., Wang, A., Zhang, H., Ding, B., Hu, Z.: Hydriding properties of a mechanically milled Mg–50 wt% ZrFe 1.4 Cr 0.6 composite. J. alloy compd. **297**, 240–245 (2000)
9. Li, F., Jiang, L., Du, J., Wang, S., Liu, X., Zhan, F.: Synthesis and hydrogenation properties of Mg–La–Ni–H system by reactive mechanical alloying. Int. J. hydrogen Energy **31**, 581–585 (2006)
10. Barkhordarian, G., Klassen, T., Bormann, R.: Kinetic investigation of the effect of milling time on the hydrogen sorption reaction of magnesium catalyzed with different Nb_2O_5 contents. J. Alloy. Compd. **407**, 249–255 (2006)
11. Wagemans, R.W.P., van Lenthe, J.H., de Jongh, P.E., Van Dillen, A.J., de Jong, K.P.: Hydrogen storage in magnesium clusters: quantum chemical study. J. Am. Chem. Soc. **127**, 16675–16680 (2005)
12. Zhu, M., Lu, Y., Ouyang, L., Wang, H.: Thermodynamic tuning of Mg-based hydrogen storage alloys: a review. Materials. **6**, 4654–4674 (2013)
13. Liang, G., Huot, J., Boily, S., Van Neste, A., Schulz, R.: Catalytic effect of transition metals on hydrogen sorption in nanocrystalline ball milled MgH_2–Tm (Tm = Ti, V, Mn, Fe and Ni) systems. J. Alloy. Compd. **292**, 247–252 (1999)
14. Barkhordarian, G., Klassen, T., Bormann, R.: Catalytic mechanism of transition-metal compounds on Mg hydrogen sorption reaction. J. Phys. Chem. B **110**, 11020–11024 (2006)
15. Dornheim, M., Doppiu, S., Barkhordarian, G., Boesenberg, U., Klassen, T., Gutfleisch, O., Bormann, R.: Hydrogen storage in magnesium-based hydrides and hydride composites. Scripta Mater. **56**, 841–846 (2007)
16. Morinaga, M., Yukawa, H.: Nature of chemical bond and phase stability of hydrogen storage compounds. Mater. Sci. Eng. A **329**, 268–275 (2002)
17. Takacs, L.: Self-sustaining reactions induced by ball milling. Prog. Mater Sci. **47**, 355–414 (2002)
18. Williamson, G., Hall, W.: X-ray line broadening from filed aluminium and wolfram. Acta Metall. Mater. **1**, 22–31 (1953)
19. Hosseini-Gourajoubi, F., Pourabdoli, M., Uner, D., Raygan, S.: Effect of process control agents on synthesizing nano-structured 2 Mg–9Ni–Y catalyst by mechanical milling and its catalytic effect on desorption capacity of MgH_2. Adv. Powder Technol. **26**, 448–453 (2015)
20. Raygan, S., Pourabdoli, M., Abdizadeh, H., Medraj, M.: Synthesizing nanostructured Ni75Mg16.66Y8.34 (at%) powder by solid state reaction and mechanical milling. Mater. Manuf. Process. **27**, 1300–1305 (2012)
21. Suryanarayana C.: Mechanical Alloying and Milling. CRC Press (2004)
22. Sakintuna, B., Lamari-Darkrim, F., Hirscher, M.: Metal hydride materials for solid hydrogen storage: a review. Int. J. Hydrogen Energy **32**, 1121–1140 (2007)
23. Shang, C., Guo, Z.: Structural and desorption characterisations of milled (MgH_2 + Y, Ce) powder mixtures for hydrogen storage. Int. J. Hydrogen Energy **32**, 2920–2925 (2007)
24. Sarussi, D., Jacob, I., Bloch, J., Shamir, N., Mintz, M.: The kinetics and mechanism of cerium hydride formation. J. alloy compd. **191**, 91–99 (1993)